E215: Particle-Antiparticle oscillations at Belle II
Lab Report

Team A5

Aarathi Parameswaran

Purbita Kole

23rd August 2023

Bonn-Cologne Graduate School of Physics and Astronomy

University of Bonn

Advanced Lab Course

Winter Semester 2023/2024

Contents

1 Introduction

The aim of this lab is to study the flavor oscillations of the neutral B meson and its antiparticle at the BELLE-II experiment at the Super-KEKB accelerator in Japan. At the accelerator, due to electron-positron annihilation heavy B meson pairs are created and other decays occur as well. The data for these decays is simulated from the BELLE-II experiment and is characterized by their imaging in the event display. The decay of the B^0 meson is reconstructed in steps of the decay chain by reconstructing the invariant mass of the particles. Finally, to study the particle anti-particle oscillation, the asymmetry function was analysed to calculate, the oscillation frequency and dilution [1] [1].

1.1 Belle II experiment and Υ(4s) events

BELLE-II detector is a part of the Super KEKB accelerator. This accelerator e^-e^+ annihilation event occurs to produce high energy events like the $\Upsilon(4s)$ at 10.579 GeV. All the data used in the analysis are measured in the lab frame. Different particle events trace different parts in the Belle detector as discussed in Sec(2.1). Although production of the $\Upsilon(4s)$ is not the most probable event of e^-e^+ annihilation.$\Upsilon(4s)$event can be easily reconstructed from the track. $\Upsilon(4s)$ has almost 50-50 branching ratio for B^+B^- and $B^0\bar{B}^0$ decay. To investigate various B meson decay modes the event was boosted in the start using two asymmetric beams of 7 GeV and 4 GeV.

1.2 Decay Chain of neutral B mesons

We study a particular neutral B meson decay chain (2) due to relatively high branching ratios and clear signature of D^* [1]. B meson decays are mostly stable to non-standard model processes and thus are very efficient for testing various effects of the Standard Model. From the $\Upsilon(4s)$ event two boosted neutral B mesons were produced in the z direction. $B^0/\bar{B}^0$ decays with a first-order weak interaction and flavour change. $B^0/\bar{B}^0$ decays are mostly hadronic (only hadrons are produced) or semi-leptonic (leptons with its neutrinos are also produced) decays. In this analysis , the decay chain of $\overline{B^0} \to D^{*+}\ell^-\overline{\nu}$ $D^{*+} \to D^0\pi^+$ $D^0 \to K^-\pi^+$ is analysed. The decay $\overline{B^0} \to D^{*+}\ell^-\overline{\nu}$ has comparatively a moderate

[1] All the particle parameter values are taken from [2]

branching ratio compared to other modes[2]. In this analysis, the invariant mass is used for the reconstruction of the decays.

1.3 Importance of $\overline{B^0}B^0$ oscillations

$\overline{B^0}B^0$ oscillations is a type of neutral meson mixing phenomenon, where neutral meson oscillates into their anti-particle. From measuring such oscillations, important parameters of the CKM matrix are determined and various symmetries of the Standard Model are analysed[3]. This phenomenon proceeds via second order weak flavour interactions. From relating the Hamiltonian and its mass eigenstates, after temporal evolution, we will see the flavour eigenstates as a superposition of the particle and anti-particle mass eigenstate [1]. As oscillations of the $\overline{B^0}B^0$ occurs mostly by exchange of virtual heavy particle, they are short distance interaction [4] So both the $\bar{B^0}B^0$ have similar decay rate and can be distinguished due to the non-zero mass difference of their physical eigenstates. The probability of find a $\bar{B^0}/B^0$ after time t is given by [1]-

$$W_{B^0/\bar{B^0}} = \frac{1}{2}\exp -\tau t(1 \pm cos(\Delta m t) \tag{1}$$

where τ is the decay rate of the particles and Δm is the oscillation frequency of the particle. In experimental analysis, a further function is derived known as the mixing asymmetry function which gives a relation between the actual particle events and the oscillation frequency (as seen in Section(2.5)).

2 Execution and Measurement

2.1 Visual Inspection of BELLE II events

The first part of the execution involves studying the event display of BELLE II events and distinguishing the different energy depositions in the tracker and the calorimeter. While the experiment aims to study the collision of e^-e^+ leading to the decay into $B^0\overline{B^0}$, there are other physical processes that occur at BELLE II. The relevant physics processes are:

1. $e^-e^+ \rightarrow \Upsilon(4S) \rightarrow B\overline{B}$
2. $e^-e^+ \rightarrow q\overline{q} \rightarrow hadrons$
3. $e^-e^+ \rightarrow e^+e^-$
4. $e^-e^+ \rightarrow \mu^-\mu^+$
5. $e^-e^+ \rightarrow \tau^-\tau^+$
6. $e^-e^+ \rightarrow \gamma\gamma$

Because different particles interact in a particular way with each layer of the BELLE II detector, we use the graphical representation of collision events to identify the decay processes and distinguish the desired decay process.

2.1.1 BELLE detector basic structure and detection capability

The detector used in BELLE II experiments consists of various types of detectors each with specialised detecting capabilities.

- **Tracker** The tracker segment in the Belle II experiment consists mainly of Vertex Detector, Central Drift Chambers and superconducting magnets. This part mostly helps in tracking the momentum and position of charged particles. Most accelerated charged particles like e^-, interact with the matter in the media through processes like ionisation or Bremsstrahlung (electromagnetic radiation produced in deceleration of a charged particle under the influence of another e^- or nuclei. Both the Vertex Detector and Gaseous Drift Chamber function on the ionisation processes, where primary ionisation due to the charged particle leads to many secondary ionisation, creating a

measurable signal. Vertex detectors are semiconductor detectors made with silicon, which are extremely precise in determining the position of decay. This is possible due to the low ionisation energy of the semiconductor and the small energy range of ionisation. Gaseous chambers though help in tracking the path of the charged particles (and other detectable) particles, lack such precise spatial resolution. Different charged particles get detected in this tracker from which charge and momentum can be calculated.[5, 6]

- **Electromagnetic Calorimeter** For charged particles and photons of high energy, a combined phenomenon of Bremsstrahlung and pair production leads to a cascade of shower or lots of secondary ionisation events. Electromagnetic detectors measure the total energy absorbed from such events. Thus high-energy particles especially photons, which are not detected in the tracker can be detected in the calorimeter.[6]

- **Particle Identification Detector(PID) or Cherenkov Detector** The PID helps in determining the mass of charged particles precisely from their momentum and the Cherenkov angle (Measured from the wavefront of radiation, due to high energy particle traversing in dielectric medium). Thus in Belle II, it serves the primary purpose of separating kaons and pions.[6, 3]

- K_L **and muon detector (KLM)** The outermost layer of the Belle II detector is for tracking the K^0long and muons, which previously might escape detection in the detector. This is realised by thick layers of iron plate surrounded by superconducting solenoid, which have active detectors located outside them.[3]

We use the knowledge that different charged particles interact differently with each layer of the detector to identify the decays in the event display as done in the following section. Electrons shower in the first layers of the calorimeter, charged hadron showers reach intermediate layers of the detector, while muons do not initiate a shower and traverse the detector and are seen in the KLM [1].

Muon Decay

The event display in Figure 1 is that of the muon decay $e^-e^+ \rightarrow \mu^-\mu^+$. This was deduced by the observation that the particles after collision leave tracks prominently in the K^0long and muon detector (KLM detector) and not in the electromagnetic calorimeter. Moreover,

the tracks were directed in opposite directions, an indication of the opposite charges of the particles.

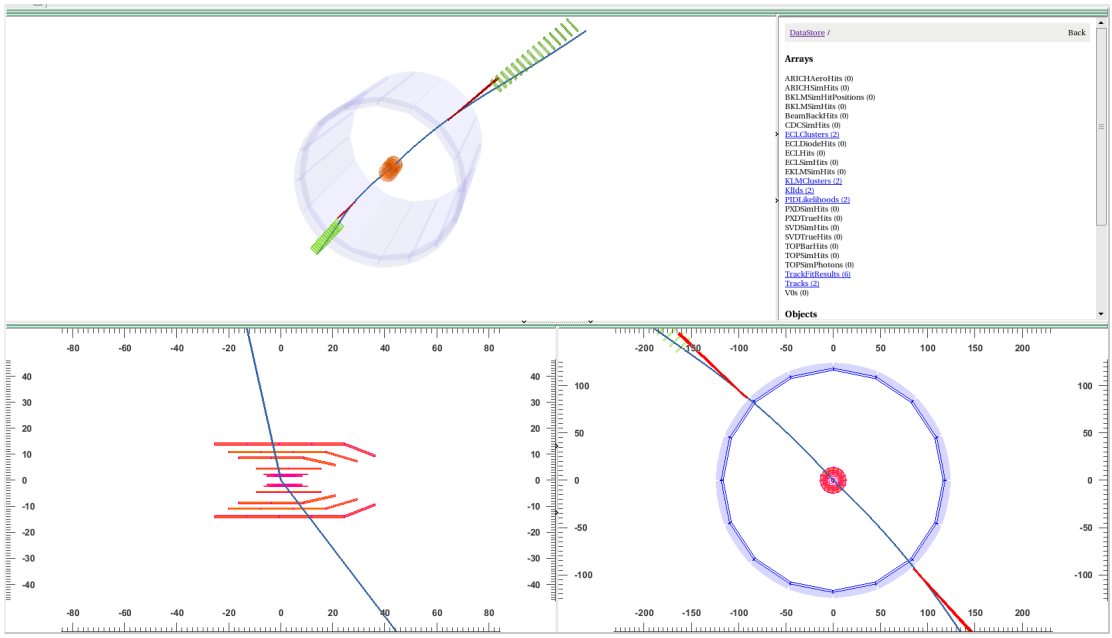

Figure 1: Event display for muon decay

Gamma decay

The event display in Figure 2 was found to be that of the gamma decay $e^-e^+ \rightarrow \gamma\gamma$ because there is no trajectory traced in the tracker, implying the presence of neutral particles, but can be seen in the electromagnetic calorimeter. Gamma rays mainly interact with matter in the form of photo-electric effects or interactions like pair production or Compton scattering. Thus the energy produced only shows up in the calorimeter. This makes it evident that it is the electron-positron annihilation leading to gamma radiation.

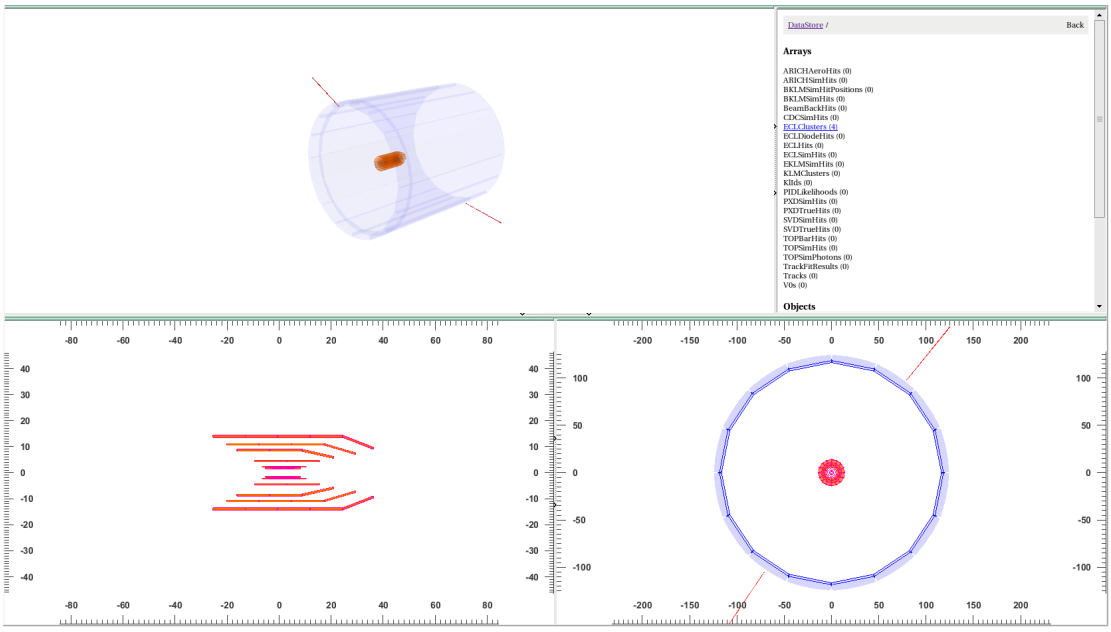

Figure 2: Event display for gamma decay

Electron-positron generation

The event display in Figure 3 corresponds to the generation of an electron-positron pair, indicated by two oppositely directed particles traced in the tracker. The lack of other decay events also implies it is the most probable decay branch i.e. electron-positron generation.

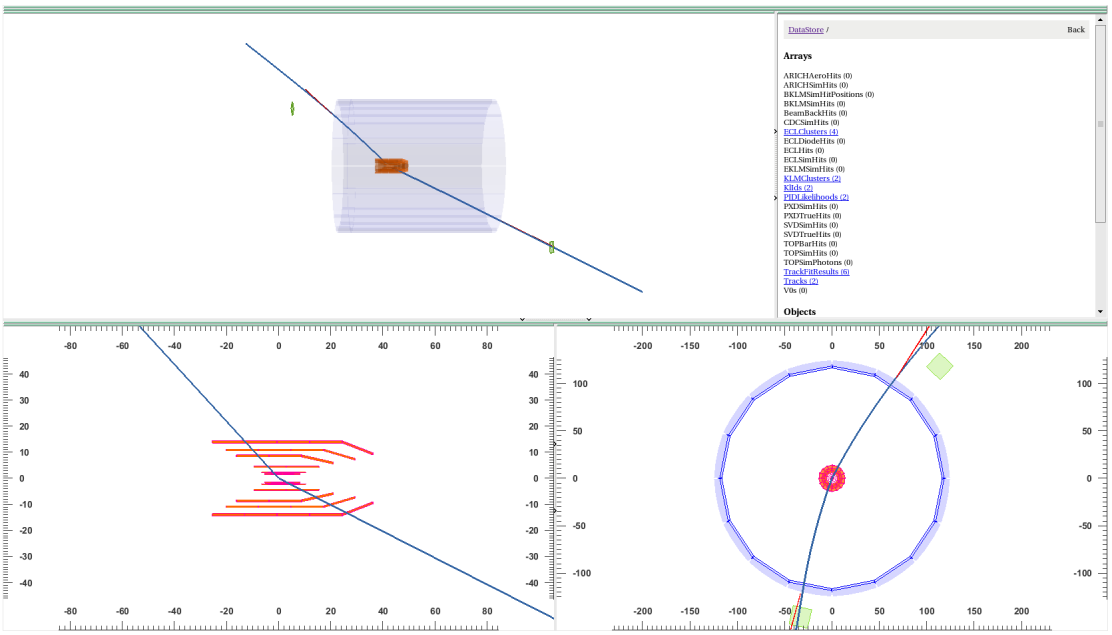

Figure 3: Event display for electron-positron pair

Tau decay

The event display in Figure 4 was found to be τ^+ τ^- decay. The tau particles are too short-lived to be decayed. Most of the tracks are found only on one side. So two oppositely directed tracks of various secondary decay indicate the τ^+ τ^- decay.

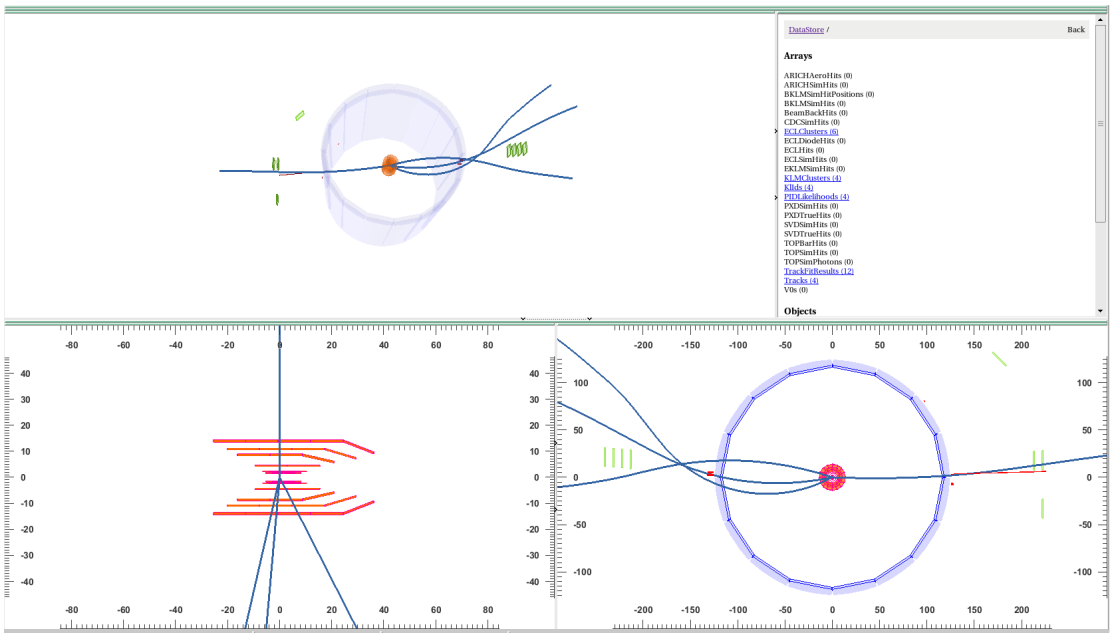

Figure 4: Event display for Tau decay

Quark decay

The event display in Figure 5 indicates the decay to the quark anti-quark pair. The $q\bar{q}$ pair quickly annihilates into two oppositely directed jets of hadrons, due to the boosts in those directions. In Figure 5, various decay processes can be seen but directed in opposite directions.

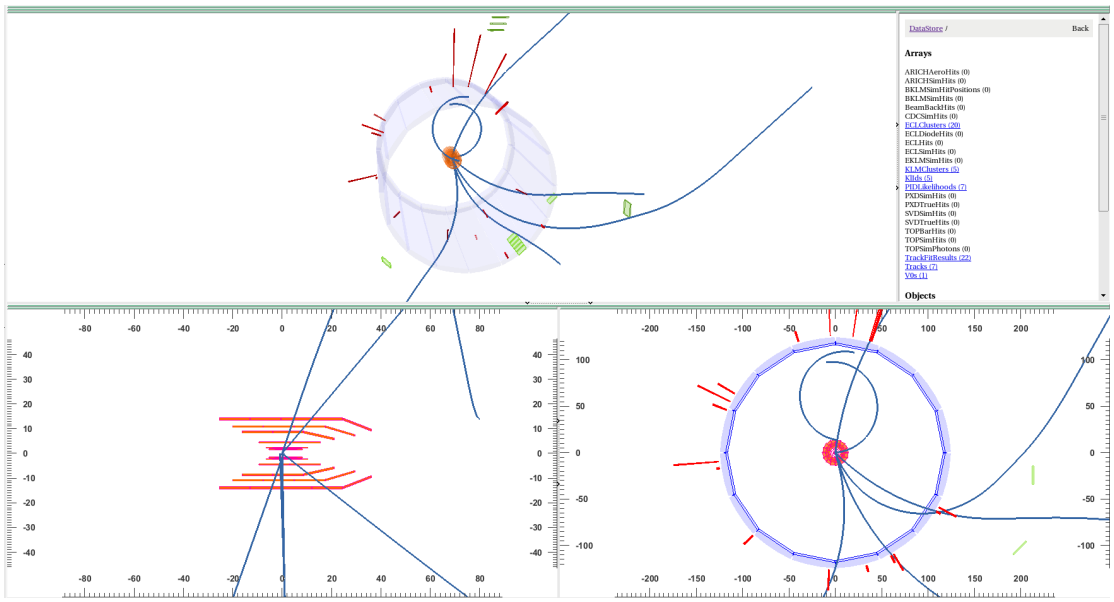

Figure 5: Event display for quark decay

B meson decay

The event display in Figure 6, shows highly deflected particles of various decay products. The particles created are deflected in a spherical manner with no specific direction. The heavy and charged products of the $B\bar{B}$, possibly create the tracks as shown in Figure 6.

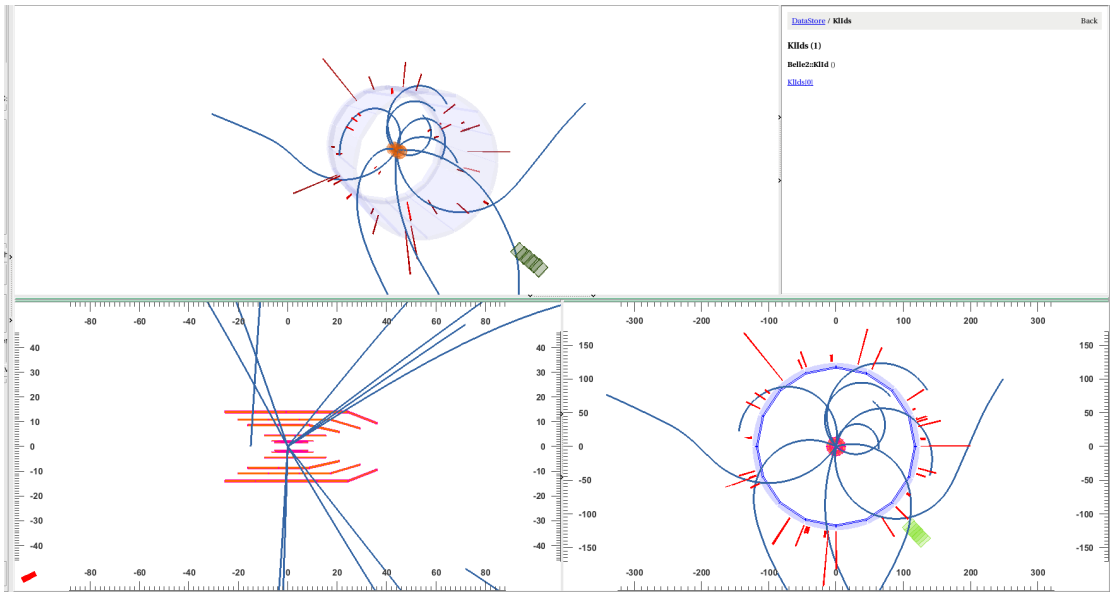

Figure 6: Event display for B meson decay

In order to investigate the $e^-e^+ \rightarrow \Upsilon(4S) \rightarrow B\overline{B}$ decay channel, the data corresponding to Figure (6) is taken. The data is analysed further to reconstruct various particle data of the $B^0\overline{B^0}$ decays. Of the many B^0 decays that occur, the one we study at BELLE II is the decay chain comprising of

$$\overline{B^0} \rightarrow D^{*+}\ell^-\overline{\nu} \quad D^{*+} \rightarrow D^0\pi^+ \quad D^0 \rightarrow K^-\pi^+ \tag{2}$$

The above decay holds for the corresponding antiparticles as well.

2.2 Reconstruction of D^0 decay

The reconstruction of the B^0 meson decay is done starting with the last step in the chain, which is the D^0 decay and the chain is traversed backwards, eliminating the background signals in each step. The background comes from particles from other decays outside of this particular decay chain and therefore, needs to be eliminated before analysis.
The D^0 is unstable and after a short lifespan decays as follows:

$$D^0 \rightarrow K^-\pi^+ \tag{3}$$

D^0 mass reconstruction

The first step involved the calculation of the invariant mass of the particles. This can be done using the conservation laws for energy and momentum. Considering the relativistic four-momentum according to the Lorentz invariance, the conservation law is stated as:

$$M^2 = E^2 - P_x^2 - P_y^2 - P_z^2 \tag{4}$$

where M is the invariant mass, E is the relativistic energy and $P_x, P_y$and P_z are the different momentum components. From this equation, we can calculate the invariant mass of the parent particle (D^0) from the energy and momentum of the daughter particles (the kaons and pions). The invariant mass of D^0 is calculated by:

$$M_{D^0}^2 = (E_{K^-} + E_{\pi^+})^2 - (P_{xK^-} + P_{x\pi^+})^2 - (P_{yK^-} + P_{y\pi^+})^2 - (P_{zK^-} + P_{z\pi^+})^2 \tag{5}$$

Using the PANDAS package in Python, the invariant masses are added as columns to the datasets and the invariant mass of D^0 along with the background is plotted as a histogram as seen in Figure (7).

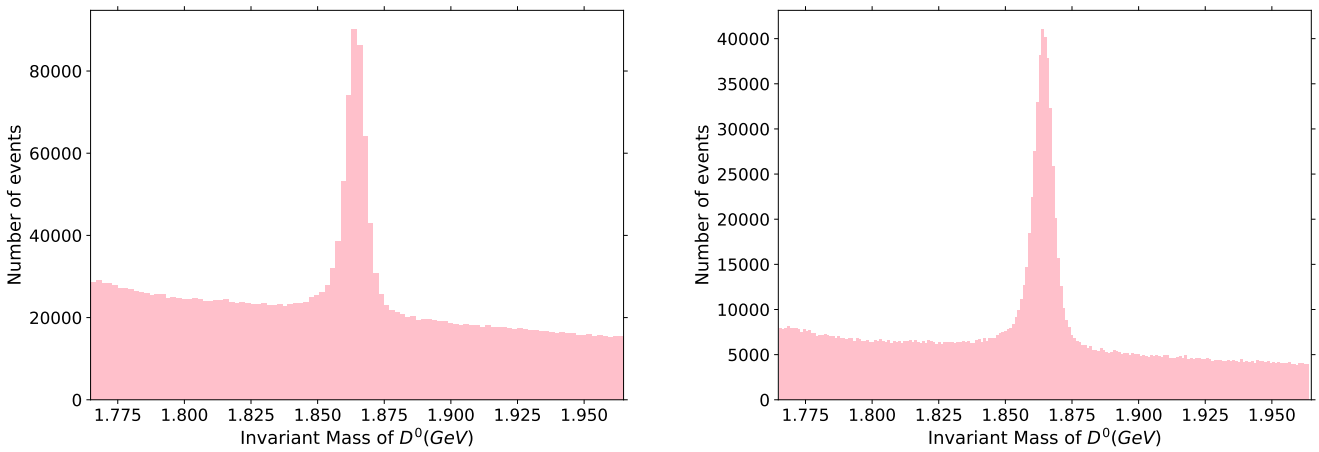

(a) Initial data

(b) After First charge cut

Figure 7: Reconstructed D^0 invariant mass from its decay products

The signal region, where the decay occurs, is indicated by the peak in the histogram where the mass of D^0 is. The regions on either side of the peak consist of the background and need to be minimised. The main obstruction in reconstructing the correct decay chain is the other probable decay branch B^+B^-. To obtain the minimised background, the first step is to perform a charge cut. These are requirements or conditions on the charges of the kaons and the pions to ensure that we only take into account the particles involved in our particular decay. From the decay equation (2), we know that the kaon and the pion should have opposite charges. So the condition applied is, that the sum of the charges of the pion and the kaon should be zero, ensuring that only the B^0 decay is considered in the analysis. The result of the first charge cut can be seen in Figure (7).

The next step for the enhancement of the signal is to perform a mass cut. For this, we first select and isolate a region as the signal region (as seen in Figure (8)). The signal region was taken within a range of 35 events around the peak. The background signal cut was chosen so as to eliminate any signal interference. The visualisation shows that the background signal almost follows a linear trend. Thus a linear fit was applied to just the background events to model it (see Figure (9)).

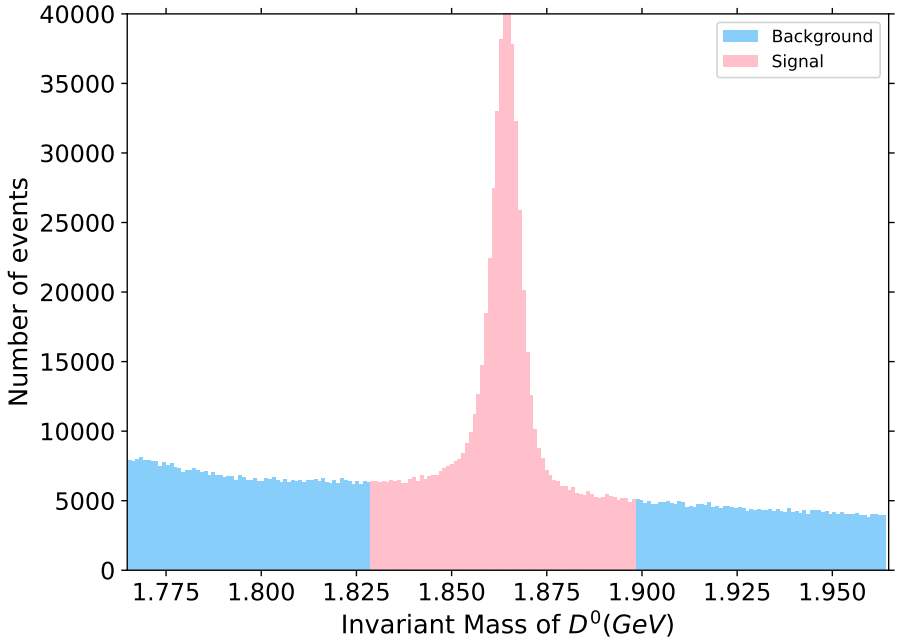

Figure 8: D^0 invariant mass signal and background events after the first mass cut

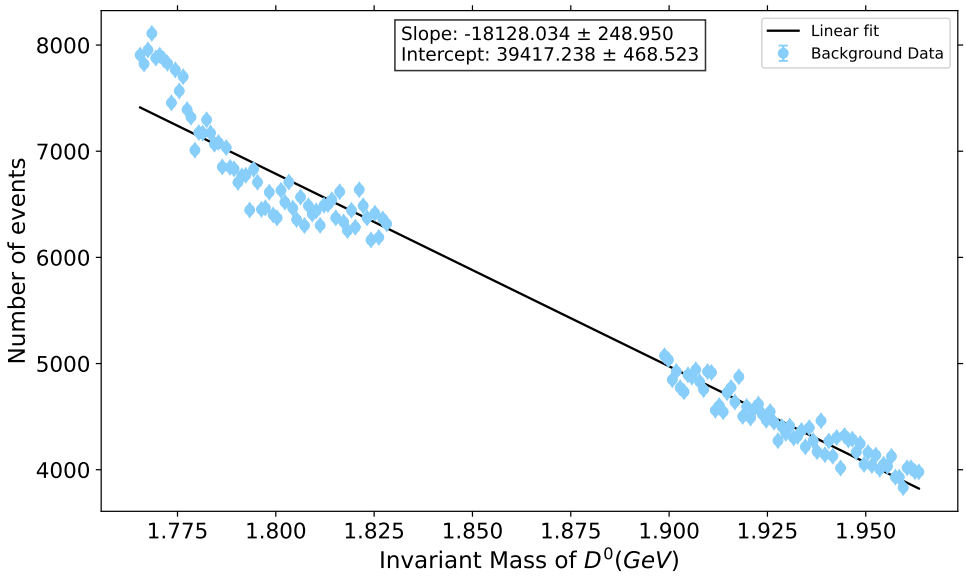

Figure 9: A linear fit is applied on the Background events of D^0 signal

After this, a second mass cut is performed just for the signal data to get an enhanced i.e. a signal-only region. The linear fit performed on the background earlier was used to estimate the background events in the signal data. This signal (see Figure (10)) to obtain it will be used for the next steps of the decay reconstruction.

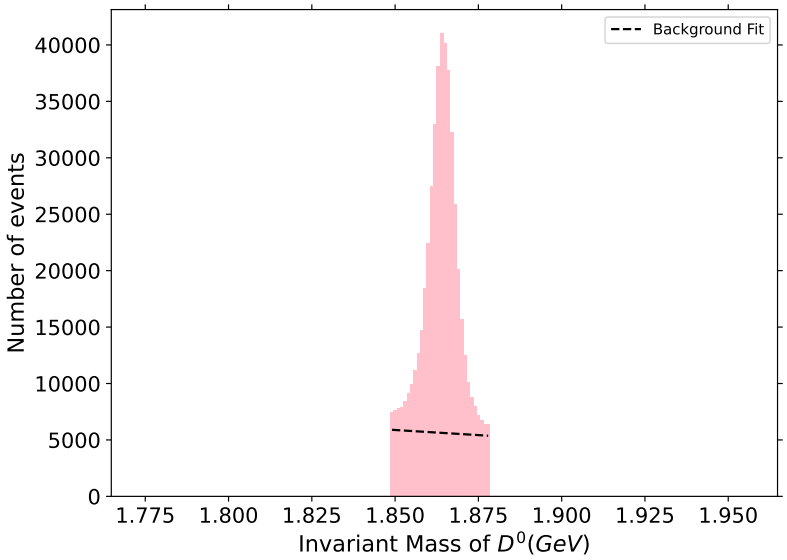

Figure 10: Caption

A quantity is used to measure the quality of signal events is compared to background known as signal purity(α), which is defined as [1]:

$$\alpha = \frac{N_{sig}}{N_{cand}} = \frac{N_{sig}}{N_{sig} + N_{bg}} = 1 - \frac{N_{bg}}{N_{cand}} \tag{6}$$

where N_{sig}, N_{bg} is the number of events in the signal and background regions, respectively. And N_{cand} is the total no of events in the signal data. As instructed for this particular task, a purity value above 65% is expected. The calculated purity for the selected data sample of the signal with enhanced D^0 content is:

$$\alpha = (\mathbf{67.21035 \pm 0.06537}\%) \tag{7}$$

where N_{bg} is calculated from summing over the linear model output applied in the final signal region[2]. The literature value of mass of D^0 is $\mathbf{1864.84 \pm 0.05 Mev}$. So as seen in

[2]with the error on purity calculated using the equation in Appendix(4.1)

Figure (10), the invariant mass is well within the range.

D^0 momentum Calculation

The next part was to calculate the average momenta of the particles. This is done using the equation:

$$P_{D^0}^2 = (P_{K^-x} + P_{\pi^+x})^2 + (P_{K^-y} + P_{\pi^+y})^2 + (P_{K^-z} + P_{\pi^+z})^2 \tag{8}$$

Using equation (8) and the equation for purity (6) we calculate the following:

- The average momentum of the combinatorial background in mass sidebands next to the D^0 mass peak is: $\mathbf{1.39029 \pm 0.0008338\ GeV}$.
- The average momentum of the D^0 particles is: $\mathbf{1.7082 \pm 0.0018\ GeV}$.[3]

D^0 mass comparison with two and three-body decay predictions

Let us first consider the two-body hadronic decay $\overline{B}^0 \to D^0\pi^0$. Consider the decay in the rest mass of $\overline{B^0}$ i.e. with a 4-momenta of the form $(M, 0, 0, 0)$. The decay products have equal and opposite momentum, due to conservation of momentum. So the energies of decay products are given by $E_1 + E_2 = \sqrt{m_1^2 + p_1^2} + \sqrt{m_2^2 + p_2^2} = M$, where 1,2 denotes the decay products and the momentum are in the rest frame of the source particle. Then the momentum of D^0 one of the decay particles is given by:

$$p_{D^0} = \frac{1}{2M_{\overline{B^0}}}\sqrt{(M_{\overline{B^0}}^2 - (m_{D^0} + m_{\pi^0})^2)(M_{\overline{B^0}}^2 - (m_{D^0} - m_{\pi^0})^2)} \tag{9}$$

From typical values adopted from [2], it is estimated the momentum of D^0 to be **2.254 GeV** in the rest frame of neutral B meson. Although there is a need to account for the boost given to the neutral meson, the momentum is still considerably higher than the one above. So the reconstructed average momentum is highly unlikely to be a result of two-body hadron decay.

Now considering the three-body decay $\overline{B^0} \to D^{*+}\ell^-\overline{\nu}$ $D^{*+} \to D^0\pi^+$. In this decay, the mass of the ν is negligible compared to the rest of the products, and the intermediate particle D^{*+} does not have a long lifetime. The limit of the momentum in the rest frame

[3]The average of momentum is calculated considering the error background, using the procedure in Appendix(4.2)

of the source particle in a three-body decay is given by [7]

$$p_{1max} = \frac{1}{2M}\sqrt{(M^2 - (m_1 + m_2 + m_3)^2)(M^2 - (m_2 + m_3 - m_1)^2} \tag{10}$$

Neutrino mass to be negligible and the lepton mass to in order of the mass of τ particle. The momentum limit calculated for D^{*+} is $\approx \mathbf{1.83GeV}$. As it decays into a slow pion and D^0, by conservation of momentum, most of the momentum should be transferred to D^0. So the estimated upper limit of momentum of D^0 for semi-leptonic decay is 1.83GeV. So the value obtained in the analysis previously is comparable to a two-step semi-leptonic decay.

2.3 Reconstruction of D^{*+} decay

This section describes the next step of the decay reconstruction involving the decay $D^{*+} \rightarrow D^0\pi^+$. This decay occurs with 68% probability and due to restricted kinematics it can be selected with high purity [1]. The pion involved in the decay is called the slow pion because the masses of the D^0 and the D^{*+} are almost similar, which makes the momentum of the pion much lower in comparison, owing to the conservation of momentum. The first task involves plotting a 2D-histogram of the D^0 momentum against the slow pion momentum. This can be seen in Figure (11).

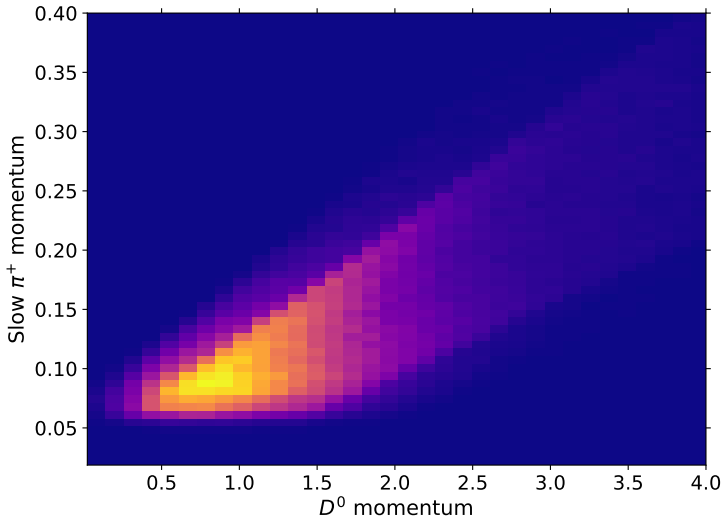

Figure 11: 2-dimensional plot highlighting the correlation between values of D^0 and slowπ^+ momentum. As seen there is a strong correlation for lower values of momentum.

From the plot, it is evident that there is a correlation between both momenta since they are products of the same decay. The following tasks involve making this correlation more prominent.

The next step involves the reconstruction of the invariant mass of the D^{*+}. This is done by calculating the total invariant mass of the three particles involved in the decay, namely the kaon, pion and the slow pion as seen in the equation:

$$M(D^{*+})^2 = (E_{K^-} + E_{\pi} + E_{slow\pi})^2 - (P_{K^-} + P_{\pi} + P_{slow\pi})^2 \tag{11}$$

Thus the histogram obtained for D^{*+} is seen in Figure (12)

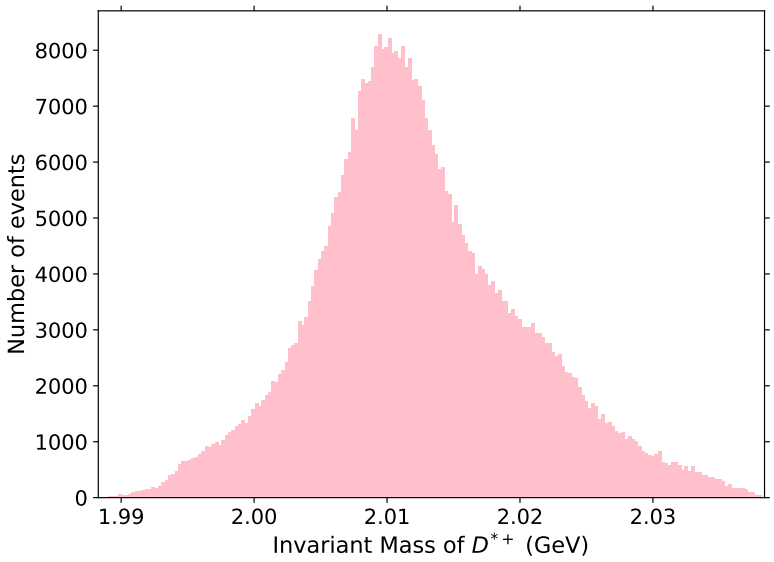

Figure 12: Reconstructed invariant mass pf $D^{*+}$from its decay products

As seen in Figure (12), the peak for the invariant mass is not as prominent because the masses of D^{*+} and D^0 are comparable. To get a more prominent peak, we plot the mass differences instead, as seen in Figure (13) and we use this mass difference as the data sample. The peak is more prominent in the plot of the mass difference because the mass difference is smaller, unlike in Figure (12).

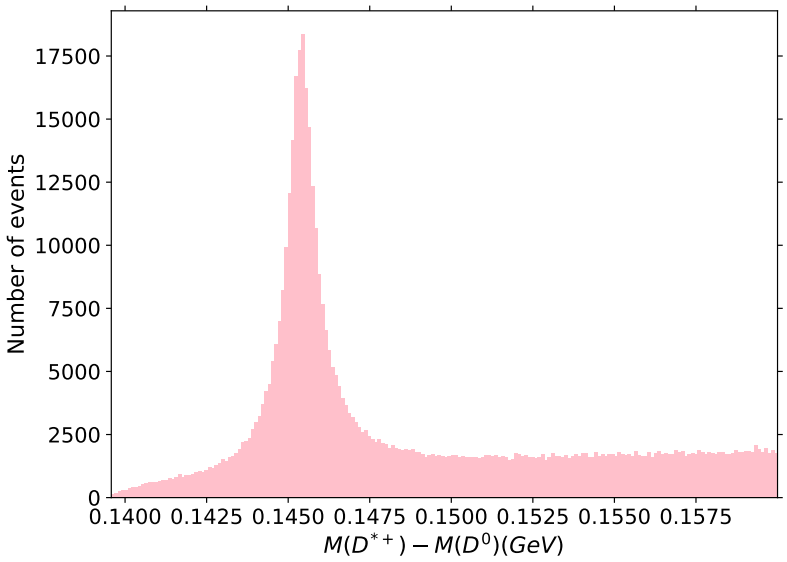

Figure 13: Invariant mass difference of D^{*+} and D^0

To this mass difference data, the charge cut applied was the condition that the charge of slow-π^+ would be the same as that of the normal π^+. This prevents considering events of similar structure from D^+ decay. Further mass cuts are applied, keeping the signal symmetric around the peak to calculate the background, shown in Figure (14).

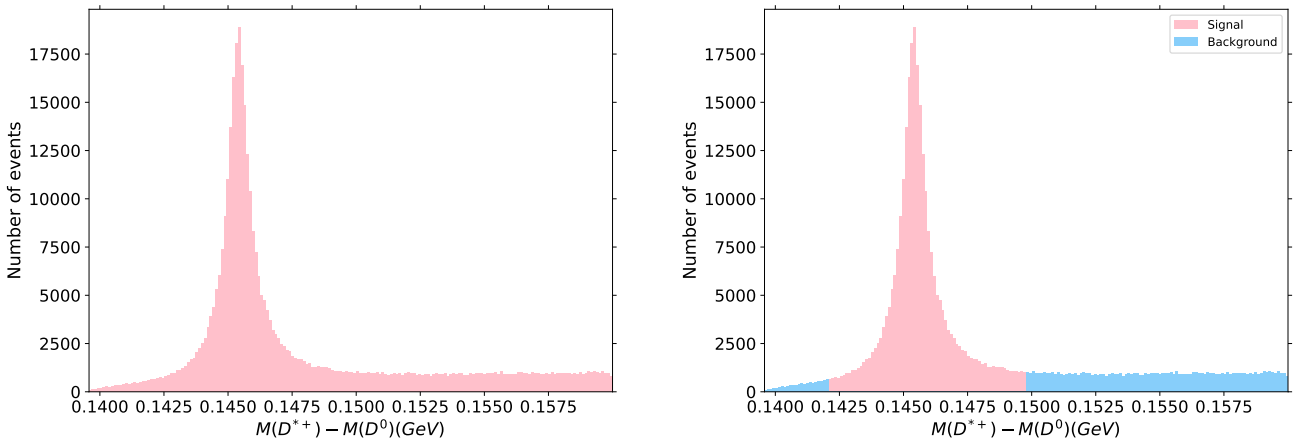

(a) Charge cut

(b) First mass cut

Figure 14: Enhanced Signal of D^{*+} mass after (a) charge cut (b) then first mass cut

A cubic polynomial fit is applied to the background signal, as in the previous section. This is seen in Figure (15).

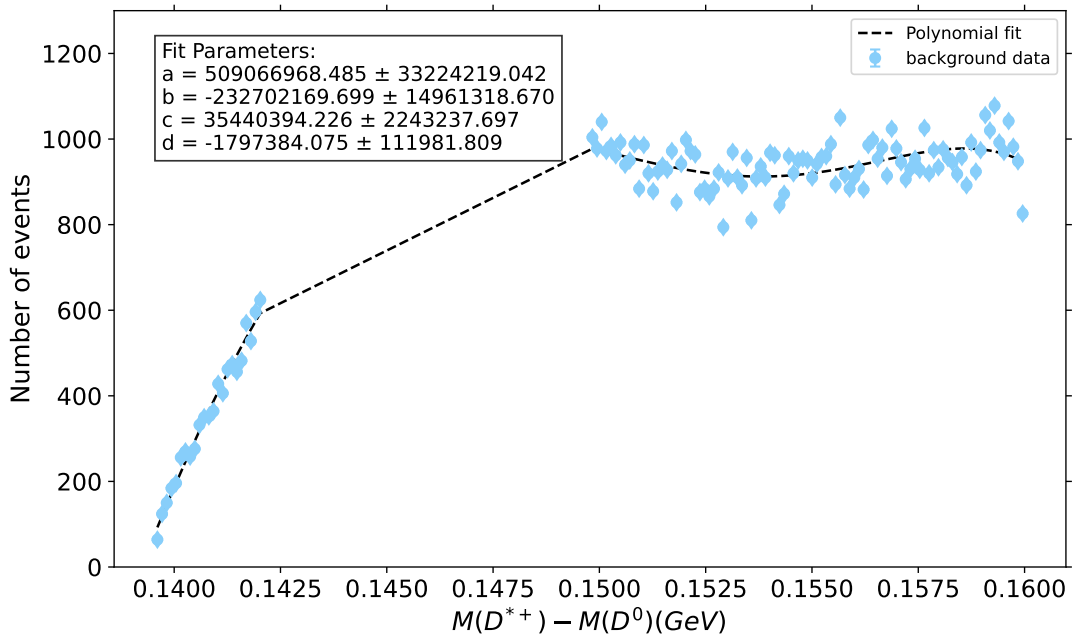

Figure 15: Cubic fit to the background signal. a,b,c,d are the coefficients of the cubic function

The second mass cut was performed taking a narrower range symmetric around the signal peak and the final signal was obtained. As expected from literature values taking $M(D^{*+}) = 2010.26 \pm 0.05$ and $M(D^0) = 1864.84 \pm 0.05$, the expected mass difference is $\mathbf{0.14542 \pm 0.00007\ GeV}$. As seen in Figure (16), the peak of the signal is well within the expected range.

The purity of the signal is calculated from equation (12) as:

$$\alpha = (\mathbf{87.6669 \pm 0.068614})\% \tag{12}$$

As stated in the manual[1], a purity above 80% is achieved.

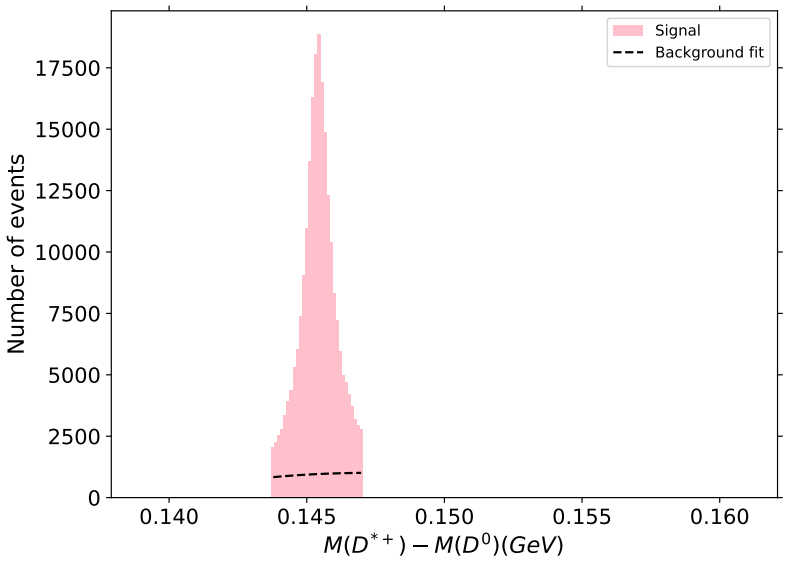

Figure 16: Reconstructed mass of D^{+*} from its signal. From the signal region background events were also estimated using the cubic fit

2.4 B^0 meson Reconstruction

In this section, we have performed the final mass reconstruction of the B^0 meson from the decay $\overline{B^0} \to D^{*+}\ell^-\overline{\nu}$ and reconstructed mass of D^{*+} from the previous section to obtain the full B meson decay chain. Here we needed to distinguish the signal leptons from the tag lepton produced from the tag B^0 meson decay. This helps in analysing data only for the signal B^0 and thus reconstructing the full decay chain.

We consider the track parameter z_0 position which gives the closest approach of the track to the beam axis and is a good approximation for the z-coordinate for the particle's point of origin. At first, we get an estimate between the signal and tag lepton point of origin by plotting a histogram of difference in z^0parameter of tag and signal lepton, as shown in Figure (17a).

The estimated z^0 position of D^{*+} meson is calculated using-

$$z_{0D^{*+}} = \frac{z_{0\pi^+} + z_{0K^-} + z_{0\pi_s^+}}{3} \tag{13}$$

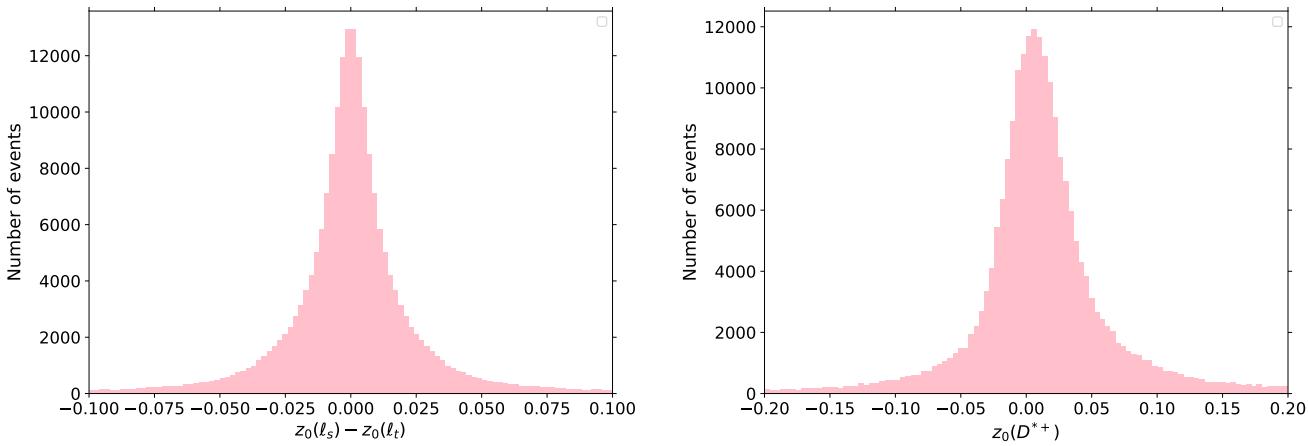

(a) Signal lepton

(b) Tag lepton

Figure 17: Distribution of z_0 parameter of the leptons in the decay

As the signal and tag leptons are not yet distinguished, the correlation diagram between the position the z_0 of D^{*+} meson and z_0 of both signal and tag lepton show high correlation (as shown in Figure (20a)). This implies that even tag leptons are falsely correlated with D^{*+} meson, as their point of origin (point of decay of parent particle) should be different. Before differentiating the data from tag and signal lepton, we calculate the invariant mass of the $\overline{B^0}/B^0$ meson (see Figure (18)), using -

$$\begin{aligned} M^2_{B^0} = (E_{K^-} + E_{\pi^+} + E_{\pi_s^+} + E_\ell)^2 - (P_{xK^-} + P_{x\pi^+} + P_{x\pi_s^+} + P_{x\ell})^2 \\ -(P_{yK^-} + P_{y\pi^+} + P_{y\pi_s^+} + P_{y\ell})^2 - (P_{zK^-} + P_{z\pi^+} + P_{z\pi_s^+} + P_{z\ell})^2 \end{aligned} \tag{14}$$

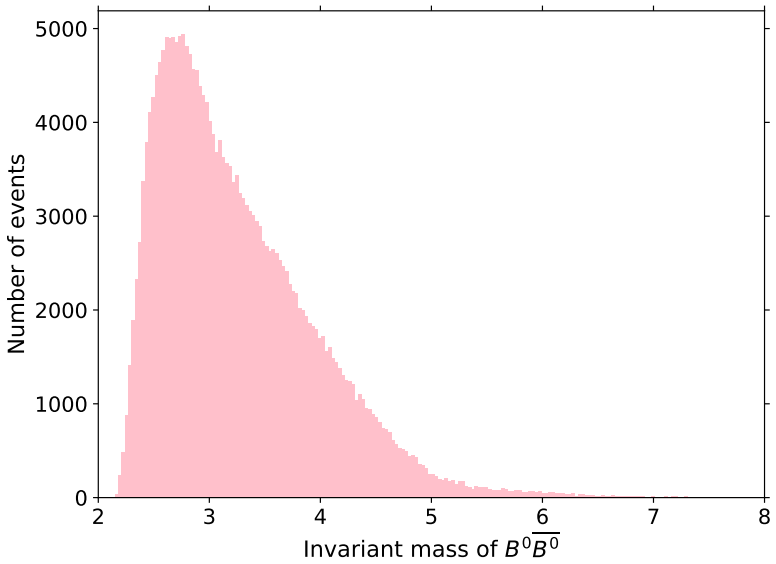

Figure 18: Reconstructed invariant mass of neutral B mesons before any signal cuts

As seen in Figure (18), the signal for the invariant mass of $\overline{B^0}/B^0$ is skewed. From the literature value, B^0 meson is predicted to have an invariant mass of $\mathbf{5279.66 \pm 0.12}$ **MeV**. This can be attributed to various reasons like counting other mesons which have such leptonic decay, counting B^+ decay etc. Thus to avoid such skewing of data and also differentiate between tag and signal meson decay, the following cuts are imposed on the data:

- The number of leptons in the event is chosen to be 2. This is to avoid other decay channels consisting of multiple tag and signal leptons.
- The ℓ charge should be equal and opposite to the charges of other decay products in the decay chain we want to reconstruct, as B^0 is neutral.
- There should be no decay chain where the invariant mass is greater than 5.27966 GeV. This is because it is impossible to expect the mass to increase as this would imply that neutrinos added extra mass.
- z^0 denotes where the particles are created during the decay. As the tag lepton would have originated from a different decay point than signal lepton the absolute difference in z^0 of tag and D^{*+} meson should be more than that between signal and D^{*+} meson.

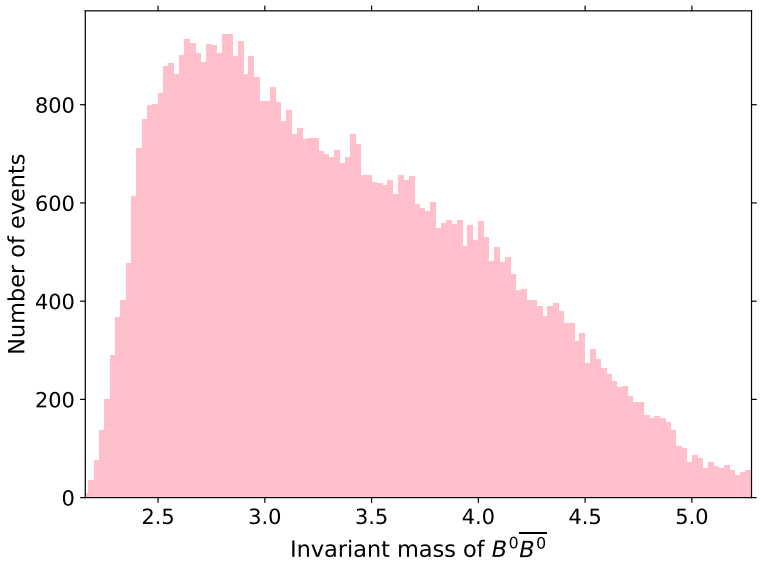

Figure 19: Invariant Mass of neutral B mesons after various signal cuts

The result of the cuts is seen in Figure (19), and we see that the data is still not symmetric about the expected mass of B^0

The 2D histograms for the z^0 of leptons against the z^0 of the D^{*+} was plotted again. From comparing the figures in Figures (20,21), we see a higher count/almost no count in the signal/tag histogram along the area where $z^0_{D^{*+}} \simeq z^0_\ell$. This shows that indeed the cuts were able to differentiate between signal and tag decay chains, up to a considerable extent.

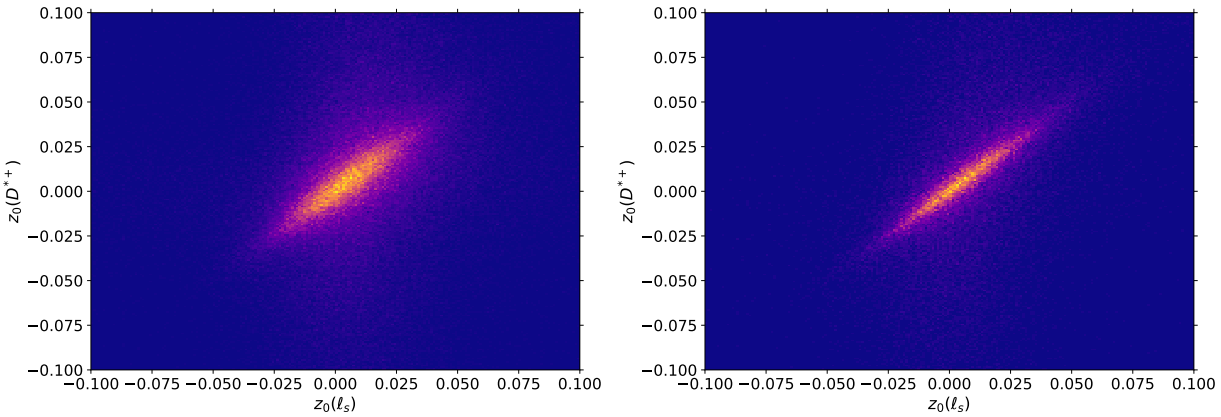

(a) Before signal cuts

(b) After signal cuts

Figure 20: Distribution of z^0 of signal leptons

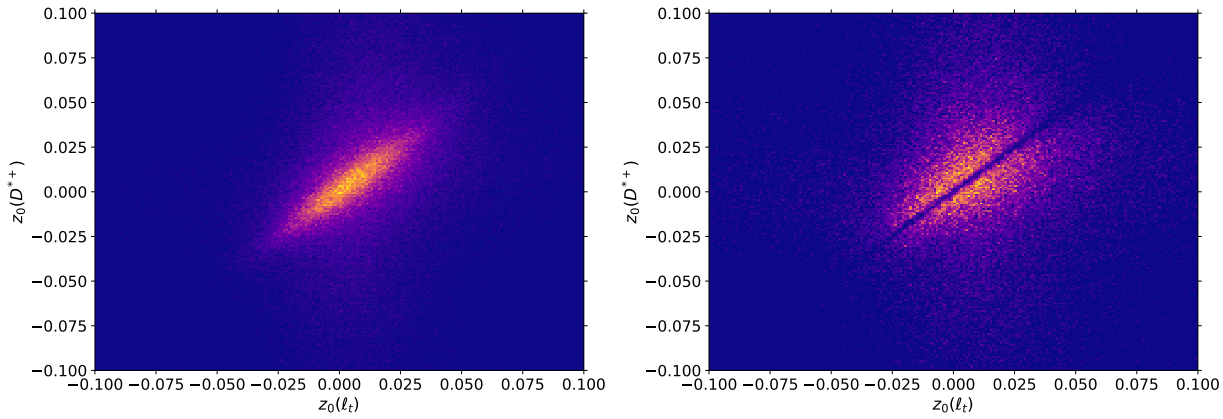

(a) Before signal cuts

(b) After signal cuts

Figure 21: Distribution of z^0 of tag lepton

2.5 Inspecting $B^0\overline{B^0}$ oscillation

As indicated in the introduction, the main motive of doing a full chain reconstruction and using the 'tagging' technique was to study the $B^0 - \overline{B^0}$ oscillations. $B^0\overline{B^0}$ oscillation was inspected using the reconstructed $B^0/\overline{B^0}$ meson (the signal data from the previous section) and the tag lepton of the other B meson ($\overline{B^0}/B^0$). Thus if the leptons had opposite charge it was counted as non-oscillated otherwise counted as oscillated. Such oscillations were studied as a function of time using the asymmetry function.

$\mathbf{B^0\overline{B^0}}$ oscillation

From $\Upsilon(4s)$ decay an entangled state of $B^0 - \overline{B^0}$ is produced. Once the first meson decays, the second meson should technically be of the opposite flavour. When the second meson decays after a considerable time, we can deduce the flavour of the second meson from its decay products. The time difference between two decay is taken as decay time. The time difference in the data is from the length difference i.e. z position difference of two events and is related by $\Delta z = \beta\gamma\Delta t$ [1].

Asymmetry Function

The Asymmetry Function is used to characterise such flavour oscillation as a function of

decay time

$$\mathcal{A} = \frac{N_{not-osci}(t) - N_{osci}(t)}{N_{not-osci}(t) + N_{osci}(t)} = cos(\Delta M t) \tag{15}$$

where ΔM is oscillation frequency (ps^{-1})

Often there is mistagging of signal or tag particles, so accordingly the function is modified to:

$$\mathcal{A} = \frac{N_{not-osci}(t) - N_{osci}(t)}{N_{not-osci}(t) + N_{osci}(t)} = (1 - 2P_{wrong})cos(\Delta M t) \tag{16}$$

where P_{wrong} is the probability of wrongly identifying either the tag or signal lepton.
The factor in equation 16 is called the dilution: $\mathcal{D} = (1 - 2P_{wrong})$ [1].

Analysing B mixing

The signal data from the previous section was separated into two sets of data, comparing the charge of signal lepton and the tag lepton. Similar sign of the lepton charge indicated, that $\bar{B^0}$ has oscillated into B^0, i.e. oscillated B meson. If the charges were opposite then it implied no oscillation.

The amplitude of the events was plotted against the decay time, as seen in Figure (22). A steady exponential decay was observed as predicted from the Eq(1). In this plotted data (Figure (22)), a further cut limiting the decay time to $12ps$ was applied. Incorrect measurement in decay time occurs due to events at higher decay times being wrongly flagged for a lower decay rate and vice versa. However, due to the exponential decay in the number of events, the events flagged incorrectly with a larger decay rate, lead to non-symmetric error and have a greater skewing effect than the events misidentified having lower decay rates. Errors also arise from the mis-identification of charged B mesons following a similar semi-leptonic decay. As such charged B mesons contribute mostly to N_{nosci} and decayed relatively slower, they skew the data more at higher decay times. So a cut was applied on the upper limit of decay time at $12ps$.[1]

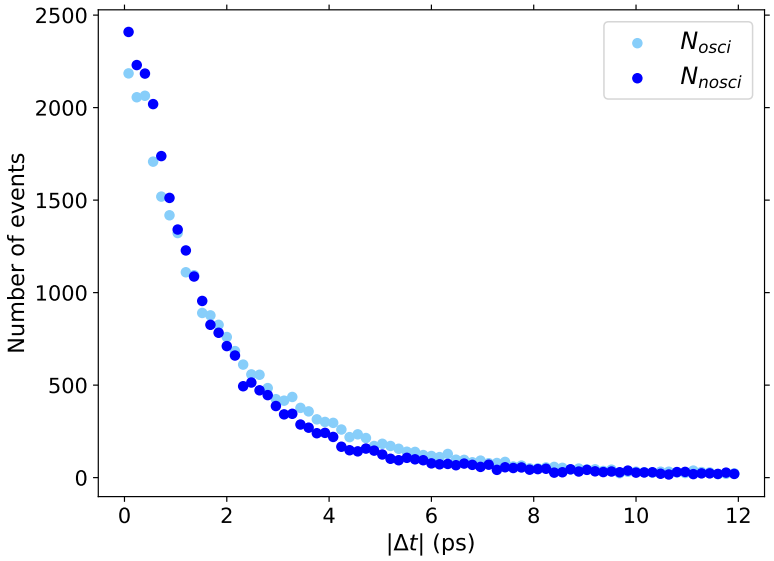

Figure 22: Plot of number of events of both oscillated nad non-oscillated B mesons vs the time in ps

The asymmetry function ($\mathcal{A}$) is computed using the Eq(15), as a function of time decay (bin-centres of 75 bins in which the final B^0 signal was distributed). The uncertainties of the function were calculated using the methods mentioned in Appendix(4.1). A cosine function of the form Eq(16) with an additional offset was fitted to the asymmetry function($\mathcal{A}$). The result of the χ^2 fit can be seen in Figure (23). From the fit and using equation (16), the parameters obtained were:

- **Oscillation frequency ΔM** $= (\mathbf{0.5212 \pm 0.018298})$ $\quad \mathbf{ps^{-1}}$
- $\mathbf{P_{wrong} = 0.4357 \pm 0.0040}$
- **Dilution Factor**$(\mathcal{D}) = \mathbf{0.12847 \pm 0.00118}$

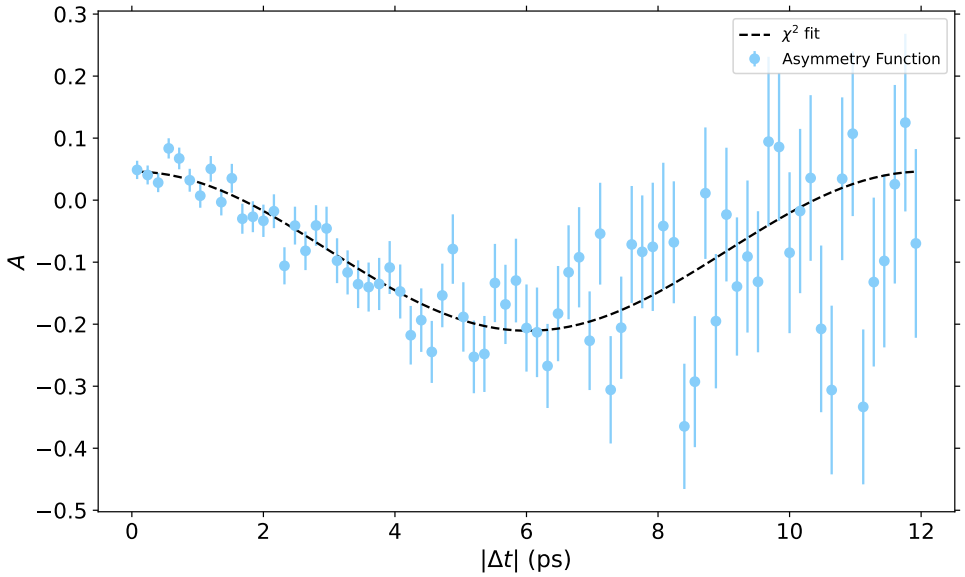

Figure 23: Asymmetry Function of mixing of neutral B mesons

The oscillation frequency obtained is comparable to available data based on the Belle experiment. The probability of falsely calculated events is also less than 50% The reduced χ^2 value was calculated to test the goodness of fit and this was found to be **1.21**, indicating a good agreement between the fit and the data.

3 Conclusion

The particle-antiparticle oscillations for the B^0 and $\overline{B^0}$ mesons as a result of the electron-positron collisions at the BELLE-II detector were analyzed through simulated data.
A simulation of the event display is studied and different decay processes that occur at the detector are observed and distinguished to identify the appropriate desired decay.
The decay process that is studied involving the B^0 meson (equation(2)) is reconstructed starting from the last chain. First the invariant mass of D^0 is plotted and using charge and mass cuts on the background, the signal is enhanced with a purity of $(\mathbf{67.21035 \pm 0.06537})\%$ is obtained.
The average momentum of the combinatorial background is $(\mathbf{1.39029 \pm 0.0008338})\mathbf{GeV}$ and the average momentum of D^0 particles is $\mathbf{1.7082 \pm 0.0018GeV}$.
In the next step of the decay, the D^{*+}, the invariant mass difference is calculated and plotted to obtain an enhanced signal of the same, with a purity of $(\mathbf{87.6669 \pm 0.068614})\%$ is obtained.
For the final step, the full B meson decay is reconstructed and z^0 positions for the D^{*+} and the signal and tag leptons are plotted. The invariant mass of $B^0\overline{B^0}$ is plotted and the data is enhanced by applying certain constraints and from the final cut dataset, we look at the correlations between the signal and tag leptons before and after the cuts.
The final dataset is then used for the asymmetry function and is used to calculate the oscillation frequency $\mathbf{\Delta M} = (\mathbf{0.5212 \pm 0.01829})\mathbf{ps^{-1}}$. Literature value?
Since the mistagging of oscillated and non-oscillated events is a source of error in the calculation, this is taken into account by calculating the probability for the same:
$\mathbf{P_{wrong}} = \mathbf{0.43576 \pm 0.004}$ and the dilution factor multiplied to the asymmetry function is $\mathcal{D} = \mathbf{0.12847 \pm 0.00118}$.

3.1 Strategies to avoid mistagging in calculating $\mathcal{A}$

In the analysis, the calculation of oscillated and non-oscillated ions may have statistical errors due to mistagging of particles. The $\mathcal{D} = 1$ presents a case where the flavour tagging is certain. But as seen here the calculated Dilution factor is quite low. This statistical error can be lowered by binning the tag signals according to their dilution[4, 8].

3.2 Other Strategies

- One can use the beam constrained mass defined by $M_{bc} = \sqrt{(E^{cms}_{beam})^2 - (p^{cms}_{beam})^2}$

  M_{bc} provides a better signal/background discrimination than the reconstructed as beam-energy resolution is smaller than the resolution of normal energy in lab frame, accounting for energy measurements of all decay products[4].

4 Appendix

4.1 Error on signal and signal Purity

The signal errors can be calculated using errors on counting number of events i.e $\sqrt{N}$, where N is the number of events. A χ^2 fit error may also be utilised in this case. The binomial error in the signal purity is given by [1]-

$$\sigma(\alpha_{purity}) = \sqrt{\frac{\alpha_{purity}(1-\alpha_{purity})}{N_{cand}}}$$

4.2 Measuring average Values in presence of Background

The background of a signal needs to be considered in order to avoid skewing the signal data. So the average of any measurement done on signal is given by [1]

$$< x_{obs} >= \alpha < x_{sig} > +(1-\alpha) < x_{bg} >$$

The errors on the average value can be calculated using the counting errors on the background and total events. This complex calculation in python is executed using UNCERTAINTIES package[9].

References

[1] *Advanced Laboratory Course physics601 E215 Particle-antiparticle oscillations at BELLE-II*. English. Version 1.3. University of Bonn, Physics Department.

[2] R. L. Workman et al. "Review of Particle Physics". In: *PTEP* 2022 (2022), p. 083C01. DOI: 10.1093/ptep/ptac097.

[3] E Kou et al. "The Belle II Physics Book". In: *Progress of Theoretical and Experimental Physics* 2019.12 (Dec. 2019), p. 123C01. ISSN: 2050-3911. DOI: 10.1093/ptep/ptz106. eprint: https://academic.oup.com/ptep/article-pdf/2019/12/123C01/32693980/ptz106.pdf. URL: https://doi.org/10.1093/ptep/ptz106.

[4] Caspar Schmitt, Christian Kiesling, and Thibaud Humair. "Background Analysis for B^0 Lifetime and Oscillation Frequency Measurement using Hadronic $B^0 \to D^{(*)-}\pi^+$ Channels at Belle II". Presented on 13 09 2021. PhD thesis. Munich: Munich, LMU, 2021.

[5] V. Luth. "Vertex detectors". In: *20th Annual SLAC Summer Institute on Particle Physics: The Third Family and the Physics of Flavor (School: Jul 13-24, Topical Conference: Jul 22-24, Symposium on Tau Physics: Jul 24) (SSI 92)*. July 1992, pp. 171–211.

[6] D. H. Perkins. *Introduction to high energy physics*. 1982. ISBN: 978-0-521-62196-0.

[7] W. von Schlippe. *Relativistic Kinematics of Particle Interactions*. https://web.physics.utah.edu/~jui/5110/hw/kin_rel.pdf. Online resource. 2002.

[8] A. J. Bevan et al. "The Physics of the B Factories". In: *The European Physical Journal C* 74.11 (Nov. 2014). DOI: 10.1140/epjc/s10052-014-3026-9. URL: https://doi.org/10.1140%2Fepjc%2Fs10052-014-3026-9.

[9] Ericnbsp; O. LEBIGOT. *Welcome to the uncertainties package¶*. URL: https://pythonhosted.org/uncertainties/.